An Analysis of Re-Entry Flight Measurements of Shock Layer Microwave Radiation

ROBERT M. NEREM* AND JOHN F. DILLEY†
The Ohio State University, Columbus, Ohio

Free-flight radiometer measurements of shock layer microwave radiation at a frequency of 2235 Mcycles/sec are analyzed from a gas-dynamic viewpoint. From these measurements, which were carried out during the re-entry of a spherical nose, 9° cone at a nominal velocity of 18,000 fps, an effective plasma temperature is defined. Although a cursory examination of the data indicates general agreement with flowfield calculations, effective temperatures as much as 1500°K higher than the equilibrium stagnation temperature were obtained in the vicinity of the sphere-cone junction. Possible mechanisms which would account for these high-temperature values are considered; and it is proposed that it is the electron temperature overshoot in the stagnation region, coupled with a nearly frozen expansion from these conditions and around the body, that produces the observed excessive plasma temperatures. Theoretical calculations of the effective plasma noise temperature for the stagnation point antenna are also presented, and reasonable agreement is obtained.

I. Introduction

ALTHOUGH the general nature of the flowfield around a blunt hypersonic vehicle is now well known, there still are many details which are not understood. This is particularly true of the physico-chemical phenomena that are present in the flow and the coupling of the associated processes with the fluid mechanic phenomena; and there is thus considerable research still in progress. This work is both of a theoretical and experimental character, and in the latter category includes free-flight as well as laboratory measurements.

The present investigation is an outgrowth of a free-flight experimental program being conducted by the Electro-Science Laboratory of The Ohio State University. This program is designed for ballistic re-entry communication studies, and the details of the particular experiment to be discussed here will be summarized in the next section.

Much of the data obtained have been from measurements of signal attenuation and reflection. However, the second vehicle in the test series was instrumented specifically for measurements of shock layer microwave radiation at a frequency of 2235 Mcycles/sec. This radiation is the result of Bremsstrahlung emission and is associated with the electron temperature of the gas. The data obtained from this flight experiment thus provides an opportunity to look at the thermal characteristics of the electrons in the flow; and it is the analysis of this data that is the subject of this paper.

As noted, the details of the free-flight experiment itself and the data will be discussed in the next section. This will be followed in Sec. III by a discussion of the nature of the shock layer surrounding the vehicle in terms of the electron characteristics. Finally, in Sec. IV comparisons will be made between the free-flight microwave radiation measurements and theoretical predictions based on both inviscid and viscous flowfield calculations.

II. Description of Experiment

The data of interest in this investigation were obtained on the second in a series of four re-entry vehicle tests.[1] The launch site for these vehicles is the NASA Wallops Island Station, Va.; and all the vehicles have been designed to telemeter data to receiving stations during re-entry with no recovery being attempted. The basic R/V configuration is shown in Fig. 1 and is a 9° blunted cone with a nose radius, R, of 0.513 ft, a length of 2.39 ft, and weighing about 65 lb.

The vehicle of interest here was launched on October 26, 1967 and was boosted upward to an altitude of 1000 kft by a two stage solid fuel rocket. Near this maximum altitude, a third stage ignited and sent the payload earthward. A fourth stage engine, located in the test vehicle itself, was then fired and accelerated the re-entry package up to a nominal velocity of 18,000 fps, or about Mach 20. The entry trajectory is shown in Fig. 2 and some of the important events during the re-entry are indicated thereon.[2]

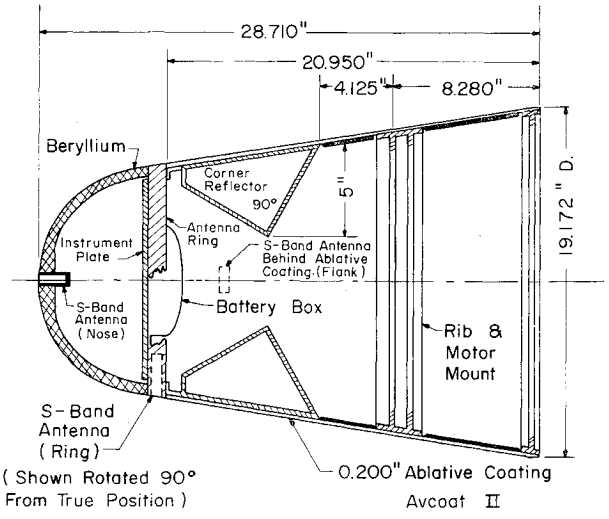

Fig. 1 Re-entry vehicle for free-flight shock layer microwave radiation measurements.

Presented as Paper 69-183 at the AIAA 7th Aerospace Sciences Meeting, New York, January 20–22, 1969; submitted February 25, 1969; revision received October 20, 1969. The authors extend their sincere appreciation to R. Caldecott, P. Bohley, and J. Mayhan of The Ohio State University ElectroScience Laboratory for the many discussions with them and for their own contributions to this effort.

* Associate Professor, Department of Aeronautical and Astronautical Engineering. Associate Fellow AIAA.

† Research Assistant, Aeronautical and Astronautical Research Laboratory; presently with General Electric Missile and Space Division, King of Prussia, Pa. Associate Member AIAA.

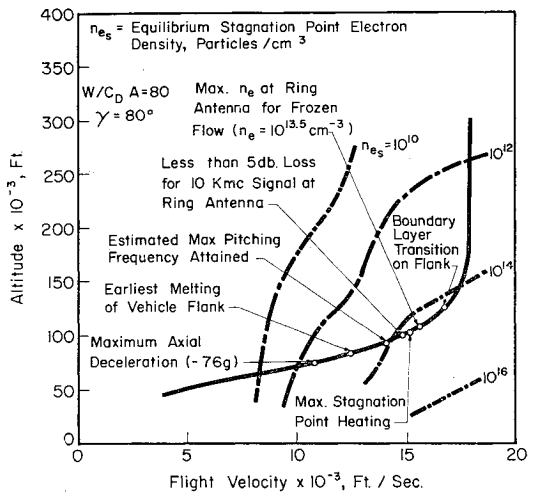

Fig. 2 Re-entry trajectory for free-flight microwave radiation experiment.

It should be noted that the vehicle was spinning at 11.4 revolutions per sec and had an angle of attack of 10.7° at an altitude of 300 kft. A heat sink type of thermal protection system was used for the nose cap with beryllium as the material; while, because of weight considerations, an ablative material, Avcoat II, was used on the flank. This choice of a thermal protection system was based on a desire to minimize impurities in the plasma and to thus obtain meaningful temperature data for a clean air plasma.

The prime piece of instrumentation on the vehicle was a radiometer operating at 2235 Mcycles/sec. Connected to the radiometer were three dielectric loaded, opened-ended waveguide, S-band antennas.[1] One antenna was at the center of the nose cap which would be the stagnation point for a zero angle of attack. Another antenna, termed here the ring antenna, was mounted in a copper ring adjacent to the nose cap at a surface distance of $S/R = 1.66$ from the stagnation point. The third antenna was positioned behind the ablative coating on the flank at a position of $S/R = 2.39$. The apparent or effective noise temperature was measured at these three antennas during re-entry. Typical flight data, consisting of the reflection coefficient and the effective plasma noise temperature, are presented in Figs. 3 and 4 for the stagnation-point and ring antennas, respectively. Since the vehicle is at an angle of attack and spinning, the data in Fig. 4 are shown for the ring antenna on the windward side of the vehicle, on the leeward side, and also amidships, i.e., at a position halfway intermediate. Although the entry nominally starts at an altitude of 300 kft., it may be seen from the data that plasma effects are not important until the vehicle reaches an altitude of about 250 kft.

It should be noted that the noise temperature data are referred to as effective plasma noise temperatures since the effect of signal reflection at the antenna has been removed. This was done by using the in-flight measured reflection coefficient. The effective plasma temperature is defined on the basis of equating the measured incident power, after correction for reflection, to that of a black body. For an isothermal slab this effective temperature would represent a minimum value for the gas (electron) temperature. This is because, for an underdense plasma, a higher temperature would be required to produce the same emitted power level; whereas for an overdense plasma, the observed temperature would be the gas temperature. However, even for a nonhomogeneous shock layer such as is of interest here, this effective temperature (which now represents an integrated effect) cannot exceed the maximum local electron temperature in that portion of the flow viewed by the antenna.

It should also be noted that a complete discussion of the accuracy of these flight measurements is contained in Ref. 1. The analysis presented there indicates that the mean deviation of the measured effective plasma temperatures is approximately 300°K. This is based on a calibration of the complete microwave receiving system and includes the use of a reflection coefficient of 0.9 (see Figs. 3 and 4) to account for reflection at the plasma-antenna interface.

Finally, a cursory examination of the data indicated general agreement between measured values for the effective plasma temperature and calculated flowfield temperatures. At the stagnation point the measured values are on the same order as the equilibrium stagnation temperature (see Fig. 3), while in the flank region the measured temperatures were considerably lower and corresponded to values typical of calculations for a chemically frozen expansion from equilibrium stagnation conditions.

However, at the ring antenna located near the sphere-cone junction, measured temperatures in excess of 6000°K and as much as 1500°K higher than the corresponding equilibrium stagnation temperature were obtained. These are shown in Fig. 4. The immediate cause of these excessively high temperature values was not apparent; and thus a more detailed analysis of all data obtained was carried out and is discussed in the remainder of this paper.

III. Flowfield Properties

The amount of shock layer microwave radiation measured by a radiometer depends on the electron density, collision frequency, and temperature distributions in the flowfield being viewed, as well as on the characteristics of the antenna. Ignoring the latter and considering only the stagnation region for the moment, it is the electron production and thermal excitation at the shock front and the boundary-layer effects that are of most interest. For the present analysis, the conditions of interest are altitudes from slightly less than 100,000 ft up to 250,000 ft, flight velocities from approximately 14,000 to 18,000 fps and shock Mach numbers from 14 to 20.[3]

Lin and his co-workers have studied the shock front ionization processes in air for this velocity range,[4,5] and the shock tube results of Ref. 4 are included in Fig. 5 where the nor-

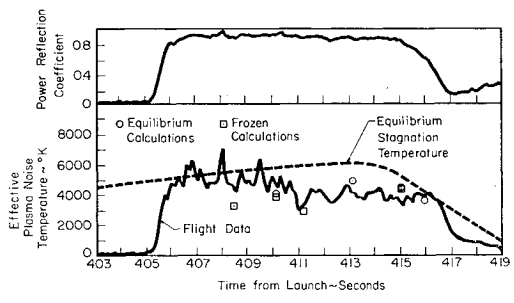

Fig. 3 Stagnation-point effective plasma noise temperature flight measurements and calculations.

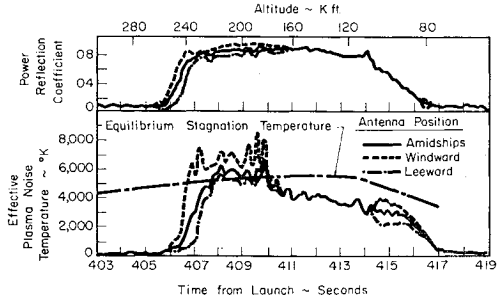

Fig. 4 Effective plasma noise temperature measurements at ring antenna near sphere-cone junction ($S/R = 1.66$).

malized ionization distance is presented as a function of shock Mach number. This ionization distance represents that required for the shock front ionization to reach a level corresponding to the equilibrium level of ionization. For the trajectory shown in Fig. 2 and accounting for the fact that in the flight case the average velocity along the stagnation streamline is approximately one-half of the velocity immediately behind the shock wave, whereas in a shock-tube experiment the velocity behind the shock wave is nearly constant, one then predicts that below 230–240,000 ft there will be sufficient time for the ionization level in the stagnation region to proceed to a near-equilibrium level such as shown in Fig. 2.

At an altitude of 240,000 ft the equilibrium stagnation point electron density[3] is approximately 2×10^{12} particles/cc, whereas at 100,000 ft the equilibrium electron density is in excess of 10.[14] For a signal frequency of 2235 Mcycles/sec (an electron density of 6.2×10^{10} particles/cc would give an equivalent plasma frequency) the stagnation region shock layer will then be overdense and optically thick to radiation. The observed microwave radiation in the stagnation region then should correspond to an effective temperature close to the equilibrium stagnation temperature, but probably being slightly lower because of the influence of the highly cooled boundary layer.

Because of this possible influence, it was of interest to carry out boundary layer calculations and include the resulting electron density, collision frequency, and temperature profiles in a theoretical calculation of the effective plasma noise temperature. For the altitudes of interest here the nature of the boundary-layer chemistry ranges all the way from frozen to equilibrium and, at the medium altitudes, is characterized by finite-rate atom and electron recombination (e.g., Ref. 6). Both frozen and equilibrium calculations for the stagnation point boundary layer thus have been carried out. These calculations are based on the assumption that the degree of ionization is sufficiently small that the basic boundary-layer characteristics, i.e., the velocity, temperature, and atom mass fraction profiles, may be determined following the theory of Fay and Riddell.[7] For the equilibrium case the resulting temperature distribution, together with the pressure, may then be used to determine the boundary-layer electron density and collision frequency profiles.[3,8]

For the frozen case, on the other hand, calculation of the electron density profile has been based on the model of Fay and Kemp.[9] Here the diffusion is assumed to be ambipolar and the $N\text{-}N^+$ charge exchange cross section large such that it is the atoms, ions, and electrons that diffuse relative to the molecules. In this case the diffusion is binary in nature, and the boundary-layer electron concentration profile is directly related to that of the atoms as may be shown using the electron specie continuity equation.[10] With the basic frozen boundary-layer characteristics determined following Ref. 7, the electron density then readily follows; and assuming the electron temperature to be equal to the gas temperature, the collision frequency may then be calculated from the simplified equation of Ref. 3. Such a boundary-layer calculation is not completely representative since the most abundant ion is NO^+ and not N^+. However, the same arguments may be advanced for the diffusion of NO, NO^+, and e^- together through the boundary layer relative to the other species. In this case the identical results are obtained if the same transport properties are used.

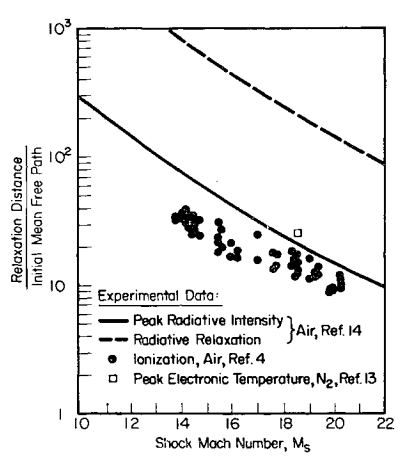

Fig. 5 Summary of experimental measurements on shock-front excitation and relaxation processes.

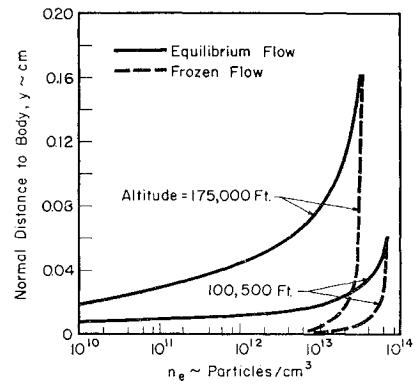

Fig. 6 Calculated stagnation-point electron density boundary-layer profiles.

Typical results from the calculations described here are shown in Fig. 6, where the stagnation point boundary-layer electron density profiles are shown for both the equilibrium and frozen cases and for altitudes of 100,500 and 175,000 ft. The respective flight velocities are 14,440 and 17,450 fps. As may be seen, there are significant differences in the electron density profile due to the nature of the boundary-layer chemistry. The temperature and collision frequency profiles have been shown, on the other hand, to be not significantly different for these two extremes in chemistry.[10] In Sec. IV, the net effect of the boundary layer and its associated chemistry on the predicted effective plasma noise temperature will be discussed.

One important aspect of the shock front physico-chemical phenomena which has not been discussed yet is the thermal excitation of the electrons and the resulting electron temperature profile. For low altitudes (high densities) the electron collision frequency is large enough that electron excitation is virtually instantaneous and the entire stagnation region shock layer will be in approximate thermodynamic equilibrium. However, for higher altitudes significant differences between the electron temperature and, for example, the heavy body translational temperature may exist in the relaxation region immediately behind the shock front.

Early studies of shock wave phenomena suggested that the electronic temperature in a diatomic gas might be strongly coupled to the vibrational temperature.[11,12] However, more recently measurements of the nonequilibrium rotational, vibrational, and electronic temperatures behind a shock wave in nitrogen have been reported by Allen in Ref. 13. These measurements were carried out at a shock velocity of approximately 21,000 fps, which is slightly above that of present interest, and at a pressure of 1 mm Hg, which is an equivalent altitude of approximately 150,000 ft. The results obtained indicate that the electronic temperature overshoots the final equilibrium temperature of 6600°K by as much as 2000°K and lies intermediate between the translational and vibrational temperatures throughout virtually the entire relaxation region. In Fig. 5 is shown the measured distance behind the shock wave at which the electronic temperature peaks. Also shown is a curve redrawn from Ref. 14 and representing measurements of the time for the radiative intensity to peak behind normal shock wave in air. As may be seen, the peak electronic temperature and the peak radiative intensity both occur at a distance behind the shock wave which is approximately equal to the previously discussed ionization distance.

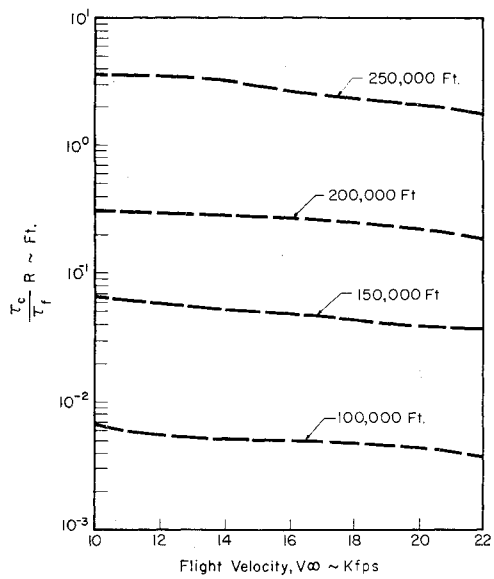

Fig. 7 Ratio of characteristic electron temperature relaxation time to characteristic flow residence time for blunt body flow.

If it is assumed that the free and bound electrons are approximately equilibrated thermally, then the peak free electron temperature also occurs at that same approximate point.

The measurements of Allen also indicate that the electronic temperature relaxes to within 10% of the equilibrium temperature in a distance of 1 cm. This is in agreement with the predicted radiative relaxation time (for the same conditions in air) obtained using the shock-tube radiative time-history measurements of Ref. 14. The radiative relaxation time is defined as the time required for the nonequilibrium radiative intensity behind a shock wave to approach within 10% of the equilibrium intensity; and a curve correlating these measurements of Ref. 14 is also redrawn in Fig. 5.

It should be noted that Allen's measurements[13] also indicate that a near-equilibrium temperature is reached in something on the order of one-half of the previously noted distance. Including this factor of two, using the radiative relaxation results of Fig. 4, and using an average velocity for the stagnation streamline, one then predicts that below approximately 165–170,000 ft near-thermodynamic equilibrium as well as chemical equilibrium conditions will exist at the stagnation point for both the electrons and the gas mixture as a whole. Below 170,000 ft one thus would expect the observed plasma temperatures to be less than the equilibrium stagnation temperature due to the effect of the boundary layer; whereas above 170,000 ft a somewhat higher temperature might be observed due to the electron temperature overshoot behind the shock front.

As the gas flows away from stagnation region and expands around the spherical nose and over the conical afterbody, electron recombination and thermal de-excitation take place. As will be seen by the results in Fig. 8, even though the electron density decreases due to recombination, the electron densities encountered still correspond to an overdense condition; and thus the radiometer measurement will only be sensitive to conditions in the immediate neighborhood of the antenna and corresponding to streamlines passing through the stagnation region.

For the velocities of interest here, the fluid mechanics of the expansion over the conical afterbody is uncoupled from the electron behavior because of the low mass fraction of the ions and electrons. However, the atom recombination processes, which are three body in nature, are important in determining the flowfield properties. For nitrogen atom three-body recombination, the characteristic atom recombination time has been calculated for flight velocities and altitudes corresponding to the range of this investigation and for a body position approximating the sonic line location. These calculations are based on the rate reported in Ref. 15; and comparing the resulting characteristic recombination time with the characteristic flow residence time, it has been found that for virtually all altitudes of interest, e.g., greater than 100,000 ft, the atom recombination is effectively frozen as the flow expands.

The electrons, on the other hand, recombine through the two-body process

$$NO^+ + e^- \rightarrow N + 0$$

for the flight conditions of interest here. The characteristic time for this reaction has been calculated using the rate of Ref. 16; and while the atom recombination is frozen, the electron recombination is neither frozen nor in equilibrium for most of the conditions of interest in this study. Thus finite-rate electron chemistry should be taken into account in any flowfield calculations.

In addition to the electron chemistry, the collisional thermal de-excitation of the electrons in this expanding flow is of interest. An upper limit on the rate at which this takes place may be estimated by defining from the electron energy equation a characteristic electron de-excitation time, τ_c, to be of the order of $(m_N/m_e\nu)$ where ν is the electron collision frequency and m_N and m_e are the nitrogen atom and electron masses, respectively. This mass ratio enters because the energy transfer in a nitrogen atom-electron collision is proportional to m_e/m_N. Evaluating τ_c based on the electron collison frequency at the sonic line location on a blunt body and approximating the characteristic flow residence time as R/V_∞, the ratio of these two characteristic times may be calculated. The result is shown in Fig. 7 as a function of flight velocity and for a number of altitudes. Assuming that electron temperatures significantly different from the heavy body translational temperature may exist when $\tau_c/\tau_f \sim 1$ or greater, then at altitudes above approximately 200,000 ft such an effect will be important for the flight velocities of interest here.

With this picture of the shock layer in mind, inviscid flowfield calculations have been carried out for equilibrium, fully frozen, and frozen flows with finite-rate electron chemistry and thermal de-excitation. These calculations use the approximate inverse method of Maslen,[17] and in the frozen flow cases are based on an expansion from assumed equilibrium postshock conditions. In the case of frozen flow with finite-rate electron processes, the atom recombination processes are assumed frozen and the basic flowfield characteristics, e.g., velocity, density, and temperature, determined. The elec-

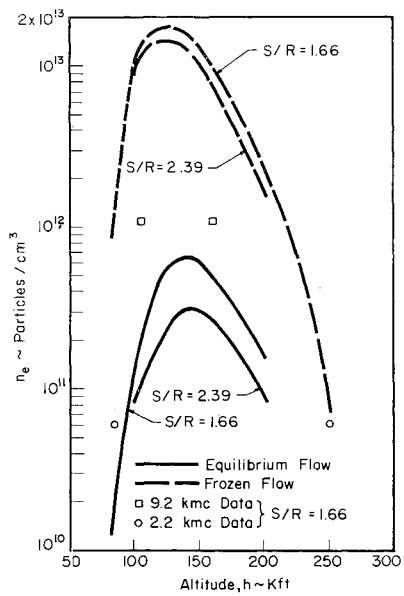

Fig. 8 Body streamline electron density calculations and flight data.

tron recombination and collisional de-excitation are then superimposed upon the streamlines of this flowfield. Typical calculations of the body streamline electron temperature distribution are shown in Fig. 9 for altitudes of 175,000 and 233,000 ft. The corresponding flight velocities are 17,450 and 17,590 fps. As may be seen, a considerable disparity between the electron and heavy body, or gas, temperatures may exist. Differences in excess of 1000°K are shown for the ring antenna location; and the electron temperature lag (behind the gas temperature) increases with increasing altitude.

It should be noted, however, that the occurrence of an electron temperature lag cannot by itself explain the temperature overshoot observed in the flight experiment since even in the absence of electron collisions with heavy bodies, the highest temperature that could exist with these calculations would be the equilibrium stagnation temperature. Thus, it would appear that to find the answer one must return to a consideration of the shock front phenomena and the influence of the associated temperature overshoot on the expanding afterbody flow. This will be discussed in the next section.

IV. Discussion of Results

Returning now to a consideration of the stagnation-point microwave data, it was pointed out in Sec. III that below an altitude of 165–170,000 ft the observed effective plasma temperature should be less than the equilibrium stagnation-point values because of the boundary-layer effect. Stagnation-point boundary-layer calculations were thus carried out as previously discussed; and the resulting boundary-layer profiles have been used to theoretically calculate the effective plasma noise temperature.

These latter calculations were performed at The Ohio State University ElectroScience Laboratory.[18] In these calculations a planar antenna, radiating into a linear, lossy, inhomogeneous media was considered, where for the present application the media is the boundary layer and the external inviscid flow. In the calculations to be presented, the boundary layer was approximated by a series of homogeneous layers (a maximum of 15 layers have been used), the properties of which are based on the calculated boundary-layer profiles. The inviscid portion of the stagnation region, on the other hand, was assumed to be uniform; and while both equilibrium and frozen boundary-layer cases have been considered, the inviscid stagnation flow was assumed to be in equilibrium for all cases.

The results obtained from these theoretical calculations are shown in Fig. 3 and compared with the earlier noted flight measurements of the stagnation-point effective plasma noise temperature as a function of time (the corresponding altitudes are also shown). Both equilibrium and frozen boundary-layer calculations are presented; and as may be seen there is quite reasonable agreement between the theoretical values and the flight data. This is particularly true at altitudes of 175,000 ft and less. Interestingly enough, at the altitudes of 100, 500, and 175,000 ft where both equilibrium and frozen boundary-layer calculations were carried out, there is no significant difference between the results for these two cases. This is in spite of the fact that the electron density profiles for these cases are quite different, as shown in Fig. 6, and that there is a noticeable boundary-layer effect. This latter is evidenced by the measured temperatures being lower than the equilibrium stagnation temperature at the altitude of 175,000 ft.

Only at the lowest altitudes at which calculations were carried out, e.g. 82,500 ft, is the measured temperature in approximate agreement with the equilibrium stagnation temperature. This is because the vehicle has by this time slowed down and is just beginning to come out of blackout for the radiometer frequency of 2235 Mcycles/sec. Furthermore, because of the high density, the boundary layer is thin, the shock layer is in virtually complete equilibrium, and the

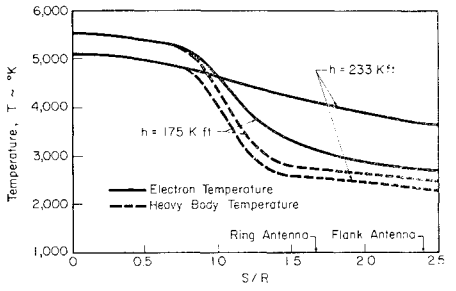

Fig. 9 Calculated body streamline electron, and heavy body temperatures for chemically frozen expansion from equilibrium stagnation conditions.

radiometer is viewing what appears to be an isothermal, equilibrium plasma slab with a plasma frequency very close to the signal frequency. The radiometer thus sees the gas temperature as modified only by reflection at the antenna-plasma interface.

The calculations for the highest altitude of 202,000 ft, on the other hand, suggest a trend to increasing temperature with decreasing altitude, whereas the data shows the exact opposite effect. It is felt that this difference is due to the fact that the calculations assume an equilibrium stagnation-point inviscid flow and neglect any effects due to electron temperature overshoot at the shock front. Because of the low densities at high altitudes, the entire shock layer may be in both chemical and thermodynamic nonequilibrium. Thus, though the boundary-layer effect by itself could cause the measured temperature to be considerably less than the equilibrium stagnation temperature, the electron temperature overshoot, which at high altitudes extends over the entire shock layer, is a compensating effect. The result is an observed temperature which is reasonably close to the equilibrium stagnation temperature for the high altitudes. Of course, above 250,000 ft the stagnation region plasma is underdense and the observed temperature rapidly decreases with increasing altitude.

The data obtained at the ring antenna location, however, are not so easily explainable. These data were presented in Fig. 4; and, as noted, for altitudes above 200,000 ft the measured temperatures are considerably higher than the equilibrium stagnation temperatures. As was discussed and shown in Sec. III, at high altitudes the electrons do not have sufficient time in expanding around the body to transfer their thermal energy to the heavy bodies, i.e., atoms and molecules, and thus an electron temperature lag develops. It was also noted, however, that such a temperature lag could not by itself explain the data; and thus that the influence of the shock front electron temperature overshoot on the expanding afterbody flow would have to be considered in the interpretation of the ring antenna noise temperature data.

Before doing this, it is of interest to compare calculated electron densities in this expanding flow region with values obtained from the flight data. Such a comparison is shown in Fig. 8 as a function of altitude. Here the calculations are for the body streamline, for both frozen and equilibrium expansions from the equilibrium stagnation conditions, and for both the ring antenna (S/R = 1.66) and flank antenna (S/R = 2.39) locations. The data for the telemetry frequency of 9.2 kmcycles has been inferred from the quality of the transmitted signal; and although complete blackout did not occur at this frequency, the vehicle appeared to be on the verge of blackout for a short period of time. Taking the beginning and end of this period and assuming that for these conditions the plasma and signal frequencies were approximately equal, resulted in the two 9.2 kmcycles values shown in Fig. 8. The 2.2 kmc data, on the other hand, are based on the power reflection coefficient time-history of Fig. 4. Here it is assumed that the onset and end of the presence of an overdense plasma, as evidenced by the sharp change in the reflection coefficient, corresponds to conditions where the signal and plasma fre-

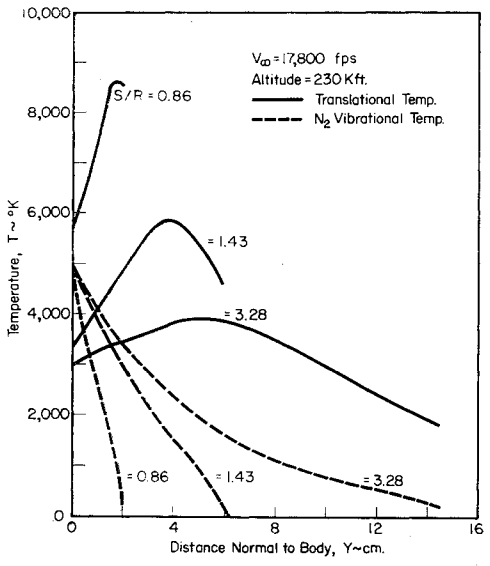

Fig. 10 Shock layer translational and vibrational temperature calculations for chemical nonequilibrium flowfield.[20]

quencies are approximately equal. It should be noted that all of the data shown were obtained at the ring antenna location.

As may be seen in Fig. 8, at the highest altitude of just under 250,000 ft, the data agrees with the frozen flow calculation; whereas at the lowest altitude, the data agrees with the calculation for an equilibrium flow expansion. At intermediate altitudes, on the other hand, the data points lie about halfway between these two types of calculations. Although this is perhaps not surprising, flowfield calculations carried out at Ohio State have indicated that this is not always the case. Thus for such intermediate altitudes the afterbody electron density is not necessarily bounded by the equilibrium and frozen cases, and may lie well below both.

Turning now to the ring antenna temperature data, it has already been noted that the shock front electron temperature overshoot and the effect of this overshoot in the downstream flow must be considered. An estimate of the peak electron temperature in the stagnation region may be made from normal shock wave nonequilibrium chemistry calculations such as presented in Ref. 19. In those calculations the electron temperature was not specifically calculated; however, an approximate value may be arrived at by assuming that the peak electron temperature is on the order of the gas translational temperature at the point in the relaxation process where the peak electron density is reached. Such an estimate does give agreement with the data of Ref. 13; and using a correlation of the previously noted calculations and taking a flight (shock wave) velocity of 18,000 fps, one arrives at a peak stagnation region electron overshoot temperature of 7700°K. This is approximately 2000 to 3000°K above the equilibrium stagnation temperature and, on the average, 1000°K higher than the observed temperatures at the ring antenna.

Furthermore, it has already been estimated in Sec. II that at altitudes above 165–170,000 ft thermodynamic and chemical electron equilibrium will not be reached in the stagnation region. Thus for altitudes of that order or higher, the shock front relaxation phenomena will be sufficiently slow so as to allow the electron temperature to peak downstream of the stagnation point. This coupled with a near frozen expansion in terms of electron temperature (such as shown in Fig. 9) could result in the excessive electron temperatures observed in the ring antenna flight data.

Now this is perhaps speculative, however an altitude of 170,000 ft corresponds to a time from launch for the present vehicle of just over 410 sec; and this is at least qualitatively in agreement with the data of Fig. 4. For smaller times, i.e., higher altitudes, excessively high temperature are observed; whereas for larger times, or lower altitudes, the observed temperatures are less than the calculated equilibrium stagnation temperatures.

It should be noted that complete chemical nonequilibrium flowfield calculations have been provided by A. B. Lewis of the USAF Flight Dynamics Laboratory.[20] These calculations were carried out using the Cornell Aeronautical Laboratory blunt body flowfield program described in Ref. 21. In this program 10 reactions and 20 species can be included; and although the electron temperature is not separately calculated, the nitrogen and oxygen vibrational temperatures are. Typical of these calculations are the inviscid shock layer temperature profiles shown in Fig. 10 for several S/R locations on the present vehicle. The flight velocity for this calculation was 17,800 fps and the altitude 230,000 ft. Shown are both the translational and nitrogen vibrational temperature profiles; and as may be seen, important differences in temperature do exist between these modes. In general the vibrational temperature lies below the translational temperature for the smallest S/R value and higher than the translational temperature, at least near the body, for the larger S/R values. This is because the vibrational temperature is virtually frozen, while the translational temperature is changing.

Normally the electron temperature behind a shock wave would peak sooner and at a higher value than the vibrational temperature and would freeze out faster once the flow begins to expand because of the m_N/m_e factor. The electron temperature then should be higher than the vibrational temperature for all S/R values. The effective plasma noise temperatures shown in Fig. 4 thus are not unreasonable, being bracketed between the electron temperature associated with a chemically frozen expansion from equilibrium stagnation conditions and the peak nonequilibrium value of the electron temperature behind the bow shock front.

It should be noted that although nothing has been said about a boundary-layer effect, there obviously should be one of similar magnitude as at the stagnation point. This should not, however, affect the preceding qualitative explanation. It should also be noted that angle-of-attack effects have not been included in this analysis. The magnitude of these effects, as shown in Fig. 4, represent only a secondary consideration.

V. Concluding Discussion

The present investigation represents an attempt to interpret re-entry flight measurements of shock layer microwave radiation from a gasdynamic viewpoint. For the stagnation-point antenna, excellent agreement has been obtained between the flight data and theoretical calculations.

For the ring antenna, the analysis carried out has been less than complete and the proposed mechanism of an electron temperature overshoot coupled with a frozen expansion is somewhat speculative. Thus, though the excessively high temperatures measured in flight can be qualitatively explained, no direct comparisons of theory and experiment were made. Nonetheless, the data provides direct evidence of ex-

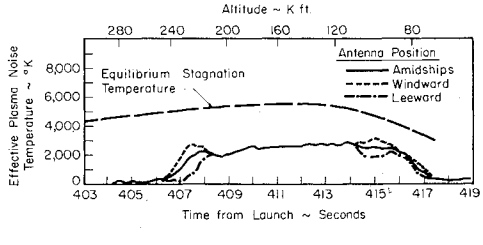

Fig. 11 Effective plasma noise temperature measurements at flank antenna (S/R = 2.39).

cessive electron temperatures in a blunt body flowfield; and the presence of this electron temperature nonequilibrium should be of importance both in re-entry communications, as well as in the observable problem.

Only the flank antenna data has not been discussed here. As noted in Sec. II and as may be seen in Fig. 11, the observed temperatures at this position were all well below the equilibrium stagnation temperature being in the range of 2000–3000°K. Although this is on the order of the translational temperatures shown in Fig. 10, undoubtedly the temperature in this region also is affected by the nonequilibrium character of the flow. An additional complexity here is the presence of ablation, the onset of which occurs for all practical purposes at 200,000 ft. Because of this additional complexity and the limited scope of this investigation, no detailed consideration has been given to these data.

References

[1] Caldecott, R. and Bohley, P., "Radio Frequency Noise During Reentry-Measurements Made at 2235 Mc/s During the Reentry of a Trailblazer Rocket Vehicle," TR 2151-7, Jan. 1968, Ohio State University ElectroScience Lab.

[2] Hartsel, J. E. and Nerem, R. M., "Predicted Reentry Performance of a Trailblazer II Vehicle," TR 1573-7, Sept. 1964, Ohio State University ElectroScience Lab.

[3] Huber, P. W., "Hypersonic Shock-Heated Flow Parameters for Velocities to 46,000 Feet Per Second and Altitudes to 323,000 Feet," TR R-163, 1963, NASA.

[4] Lin, S. C., Neal, R. A., and Fyfe, W. I., "Rate of Ionization in Air. I. Experimental Results," *The Physics of Fluids*, Vol. 5, Dec. 1962, pp. 1633–1648.

[5] Lin, S. C. and Teare, J. D., "Rate of Ionization Behind Shock Wave in Air. II. Theoretical Interpretation," *The Physics of Fluids*, Vol. 6, March 1963, pp. 355–374.

[6] Rose, P. H. and Stankevics, J. O., "Stagnation-Point Heat Transfer Measurements in Partially Ionized Air," *AIAA Journal*, Vol. 1, No. 12, Dec. 1963, pp. 2752–2763.

[7] Fay, J. A. and Riddell, F. R., "Theory of Stagnation Point Heat Transfer in Dissociated Air," *The Journal of the Aerospace Sciences*, Vol. 25, Feb. 1958, pp. 73–86.

[8] Hochstim, A. R., "Gas Properties Behind Shocks at Hypersonic Velocities. I, II, III, IV," Repts. Z-002, 003, 004, 005, Jan. 1957-Aug. 1958, Convair, San Diego, Calif.

[9] Fay, J. A. and Kemp, N. H., "Theory of Stagnation-Point Heat Transfer in a Partially Ionized Diatomic Gas," *AIAA Journal*, Vol. 1, No. 12, Dec. 1963, pp. 2741–51.

[10] Dilley, J. F., "Analytical Flow Predictions Including Non-Equilibrium Around a Re-entering Trailblazer Vehicle," M.Sc. thesis, 1968, Department of Aeronautical and Astronautical Engineering, The Ohio State University.

[11] Faizullov, F. S., Sobolev, N. N., and Kudryavtsev, E. M., "Spectroscopic Investigation of the State of the Gas Behind a Shock Wave, III," *Optics and Spectroscopy*, Vol. 8, April 1960, pp. 400–404.

[12] Keck, J. C., Camm, J. C., Kivel, B., and Wentink, T., Jr., "Radiation From Hot Air. Part III," *Annals of Physics*, Vol. 7, Jan. 1959, pp. 1–38.

[13] Allen, R. A., "Non-Equilibrium Shock Front Rotational, Vibrational and Electronic Temperature Measurements," NASA, Contractor Rept. CR-205, April 1965, Avco-Everett Research Lab., Everett, Mass.

[14] Allen, R. A., Rose, P. H., and Camm, J. C., "Nonequilibrium and Equilibrium Radiation at Super-Satellite Reentry Velocities," Rept. RR 156, Sept. 1962, Avco-Everett Research Lab. Everett, Mass.

[15] Wray, K. L., Teare, J. D., Kivel, B., and Hamerling, P., "Relaxation Processes and Reaction Rates Behind Shock Fronts in Air and Component Gases," *Eighth International Symposium on Combustion*, Williams and Wilkins, 1962, pp. 388–393.

[16] Sutton, E. A., "The Chemistry of Electrons in Pure Air Hypersonic Wakes," AIAA Paper 68-200, New York, Jan. 22–24, 1968.

[17] Maslen, S. H., "Inviscid Hypersonic Flow past Smooth Symmetric Bodies," *AIAA Journal*, Vol. 2, No. 6, June 1964, pp. 1055–1061.

[18] Mayhan, J. W., "The Calculation of the Effective Noise Temperature of Planar Antennas Radiating Into Linear, Inhomogeneous Plasma Media," Rept. 2146-10, Aug. 1968, Ohio State University ElectroScience Lab.

[19] Nerem, R. M., Carlson, L. A., and Hartsel, J. E., "Chemical Relaxation Phenomena behind Normal Shock Waves in a Dissociated Freestream," *AIAA Journal*, Vol. 5, No. 5, May 1967, pp. 910–916.

[20] Lewis, A. B., private communication, Sept. 1968, USAF Flight Dynamics Lab., Wright-Patterson Air Force Base.

[21] Curtis, J. T. and Strom, C. R., "Computations of the Non-Equilibrium Flow of a Viscous, Radiating Fluid About a Blunt Axisymmetric Body," TR AFFDL-TR-67-40, June 1967, Air Force Flight Dynamics Lab.